Comparison of All Sites for Ti Substitution in Zeolite TS-1 by an Accurate Embedded-Cluster Method

Ramesh Ch. Deka,[†,‡] Vladimir A. Nasluzov,[‡,§] Elena A. Ivanova Shor,[§] Alexei M. Shor,[§] Georgi N. Vayssilov,[||] and Notker Rösch*[,‡]

Department Chemie, Technische Universität München, 85747 Garching, Germany, Institute of Chemistry and Chemical Technology, Russian Academy of Sciences, 660049 Krasnoyarsk, Russian Federation, and Faculty of Chemistry, University of Sofia, 1126 Sofia, Bulgaria

Received: January 5, 2005; In Final Form: October 27, 2005

We studied the preferential location of Ti centers in the framework of the Ti-containing MFI zeolite TS-1 using a hybrid DFT/MM embedding method developed recently. This "covalent elastic polarizable environment" (covEPE) cluster embedding allows a complete and self-consistent treatment of solid covalent systems such as zeolites. For the present study, we used a gradient-corrected density functional approach. The resulting structural features of both Si- and Ti-substituted forms of the zeolite framework fit well with available experimental information. The calculated substitution energy of Ti at the 12 crystallographically different tetrahedral sites of the MFI structure vary within 19 kJ/mol with T12 and T2 as most and least preferred sites, respectively. On the basis of these computational results and the preferential sites for Ti substitution reported from different experimental investigations, we concluded that the Ti distribution in the TS-1 framework is not governed by the thermodynamic stability of the pure material.

1. Introduction

Transition-metal ions incorporated in the framework of a zeolite are known to induce unique catalytic properties related directly to the redox behavior of these metal ions as well as indirectly to the specific local structure and the acid properties of the zeolite framework.[1,2] The discovery of the MFI-based titanosilicalite, TS-1,[3] and its remarkable catalytic properties opened a novel route to selective hydrocarbon oxidation using H_2O_2 and other peroxide reagents.[4,5] Ti-free MFI-type silicalite material does not show a comparable catalytic performance, and therefore, the Ti atoms have been recognized as the active centers of the material. Since the discovery of Ti silicalite, various experimental techniques have been applied to characterize the structure of the titanium centers accurately.[4−12] These studies have established that at low concentration Ti occupies tetrahedral (T) sites of the zeolite framework by replacing isomorphously Si atoms of the MFI framework at [TO_4] sites; active Ti centers are well separated from one another. Subsequent computational studies[13−24] confirmed these experimental findings. However, an issue important for understanding the stability and catalytic properties of the material is still open, namely, the distribution of the Ti atoms over the structurally different, independent T sites of the MFI framework.

The monoclinic MFI zeolite features 12 crystallographically distinct T sites,[25] which we will refer to as T1−T12, following the notation of van Koningsveld et al.[26] Thus far, it is not clear whether the Ti ions are distributed randomly among all 12 T sites or whether they preferentially occupy some of the positions. Attempts to use X-ray diffraction techniques, including high-resolution synchrotron studies, for determining the preferential siting of Ti in TS-1, have been hindered by the low concentration of Ti in the framework and the poor contrast between Si and Ti centers. A low-temperature XRD study[27] indicated that likely about half of the total Ti content is located at sites T10 and T11, whereas the remaining half is probably spread among sites T1−T3 and T5−T9; sites T4 and T12 were found not to be populated by Ti. A nonrandom distribution of Ti centers in TS-1 was also reported in powder neutron diffraction studies. In particular, Lamberti et al.[28] found Ti atoms to occupy T6, T7, and T11 sites with highest probability. In a similar study, Hijar et al.[29] detected Ti substitution for Si at T3, T7, T8, T10, and T12 positions, whereas Henry et al.[30] reported T8, T10, and T3 sites as most preferred for incorporating Ti centers in the MFI lattice. As summarized in Table 1, different experimental studies unfortunately provide different selections of preferred sites for Ti substitution in MFI.

Previous theoretical studies of TS-1 employed both molecular mechanic energy minimization and structurally constrained quantum chemical approaches to predict the preferred location of Ti in the MFI framework. Sastre and Corma,[31] minimizing a force-field-based classical energy expression (molecular mechanics, MM) of orthorhombic MFI, identified T8 as the favored site and gave an energy range of 16 kJ/mol for the different T sites. Using molecular dynamics (MD) simulations, Oumi et al.[15] studied the anisotropic lattice expansion of MFI upon substitution of titanium at different lattice positions; comparing to earlier experiments,[32] they also proposed T8 as the favorable substitution site. In a similar study, Smirnov and van de Graaf[17] did not find a preferable site for Ti substitution. Njo et al.[18] used a combined MC/MM (Monte Carlo/MM) approach and identified T12 as the preferential site. Millini et al.[13] carried out density functional calculations on cluster models of fixed geometry and did not find any clear energetic preference for Ti substitution; the relative energies of the substitution sites

* Corresponding author. E-mail: roesch@ch.tum.de.
[†] On leave from Department of Chemical Sciences, Tezpur University, 784028 Assam, India; e-mail: ramesh@tezu.ernet.in.
[‡] Technische Universität München.
[§] Russian Academy of Sciences.
[||] University of Sofia.

10.1021/jp050056l CCC: $30.25 © 2005 American Chemical Society
Published on Web 12/02/2005

TABLE 1: Preferential Sites of Ti Substitution in the MFI Lattice from Experimental and Computational Studies (Arranged in Order of Decreasing Populations)

	method[a]	preferential sites	ref
exptl	XRPD	T4, T5, T11, T12	8
	XRD	T10, T11	27
	NPD	T6, T7, T11	28
	NPD	T3, T7, T8, T10, T12	29
	NPD	T8, T10, T3	30
comp	LDA[b]	T12, T3, T10, T11	13
	MD	T8[c]	15
	MC/MM	T2, T12, T7, T11	18
	MM	T8, T9, T7, T6	31
	MM	T7, T11, T12, T5	20
	QM-pot(HF:MM)	T8, T7, T5[d]	20
	ONIOM(B3LYP:B3LYP)[e]	T9, T10, T12, T1	23
	covEPE(BP:MM)	T12, T5, T7, T8	pw[f]

[a] XRPD, X-ray powder diffraction; XRD, X-ray diffraction; NPD, neutron powder diffraction; LDA, local density approximation; MD, molecular dynamics; MC, Monte Carlo method; MM, molecular mechanics; ONIOM, N-layer integrated molecular orbitals and molecular mechanics method; QM-pot, hybrid quantum mechanics/potential function method; covEPE, covalent elastic polarizable environment method. [b] With fixed geometry of the QM cluster. [c] Only this position is suggested. [d] Only these selected sites were modeled at this level. [e] Single-point ONIOM(B3LYP/Lanl2dz:B3LYP/Lanl2mb) calculations at ONIOM(B3LYP/Lanl2dz:UFF) geometries. [f] Present work.

spanned a range of about 12 kJ/mol. Sauer and co-workers[20] used an MM approach based on a force field that had been parametrized on quantum chemistry results; they calculated the maximum energy difference, 11 kJ/mol, between the lowest-energy T7 and the highest-energy T9 positions. They also carried out more elaborate QM-pot embedded-cluster calculations, but only for three selected crystallographic sites, where they found a different ordering of the site stabilities and twice larger energy differences.[20] The only comprehensive QM/MM study[23] where all T sites have been investigated was based on a rather small QM model, TO_4, containing only one T atom. This minimal QM model yielded rather small Ti−O−Si angles and Ti−O distances that were ∼5 pm shorter than the experimental values.[23]

From this overview of computational studies, one notes that the predictions of the most favorable sites for Ti substitution in TS-1 vary from one calculation to another. Apparently, just as the case in experimental studies, available theoretical approaches *failed* to provide a consistent picture of preferential siting of Ti in TS-1 zeolite. However, these theoretical methods are not free from obvious drawbacks and, therefore, their results cannot be considered as final. In particular, the accuracy of a molecular mechanics method depends strongly on the parametrization of the force field whose transferability is often difficult to control. Earlier high-level quantum chemistry calculations on cluster models with constrained geometry neglected the elasticity and the polarizability of the system under consideration. However, even the more recent hybrid QM/MM (quantum mechanics/MM) calculations employing the ONIOM[23] or the QM-pot[20] methods did not explicitly account at the QM level for the electrostatic interactions, which are included only at the classical level.

In the present study, we present the first *systematic* theoretical investigation of the substitution of Si by Ti atoms at all 12 different crystallographic positions of MFI with an *accurate* QM/MM scheme that accounts for all essential embedding effects. For this purpose, we utilized the new cluster-embedding approach in an elastic polarizable environment (covEPE),[33] which was specially developed for describing zeolites and oxides featuring covalent bonding. In this approach, a QM cluster is considered as a defect in a lattice described by the Mott−Littleton method.[34] In the covEPE scheme, the QM and the MM parts of the hybrid system can polarize each other. Also, a specially parametrized molecular mechanics force field is used and the QM/MM border region is constructed in a particular way so that one is able to relax all degrees of freedom of the combined system, composed of the QM cluster and its MM environment. In this way, one avoids artificial steric constraints on the geometry of the active center. Moreover, the covEPE scheme explicitly accounts for the electrostatic influence of the periodic zeolite lattice on the electron distribution in the QM cluster. The efficiency and the accuracy of the covEPE model was demonstrated recently by modeling the influence of the Al content and the zeolite structure on the Brønsted acidity of zeolites.[35]

2. Method

2.1. Description of the covEPE Method. Providing an adequate treatment of both the active center and its environment presents one of the main difficulties in accurate modeling of zeolites. The problem is twofold. First, an accurate model of the active center has to be used, and second, steric constraints and long-range interactions of the environment have to be included in the model. Assuming an artificially imposed periodicity, a QM supercell approach can be invoked. However, this technique is currently limited to zeolite with a relatively small unit cell.[36] Also the effects of artificially imposed periodicity on the polarization of the environment of the active center are difficult to control. In this regard, it is worth mentioning that a full QM treatment of a Ti-containing MFI lattice is very time-consuming because of the large unit cell that contains 288 atoms, among them scarcely distributed impurity Ti centers.

Alternatively, relatively simple MM methods accommodating the shell model scheme to account for the ionic polarizability have traditionally been successful in describing both perfect periodic and defective structures of zeolite materials.[37,38] Therefore, such a method is well justified for treating the environmental part of the zeolite system in the embedded-cluster approach. However, to achieve a high level of accuracy, one has to supplement this method with appropriate boundary conditions that need delicate tuning. The covEPE approach developed recently,[33] to be used in the following, fulfills all of these requirements.

In the covEPE method, one partitions the system into two regions: the active center of the zeolite, which is treated in the following with a density functional (DF) method, and the remainder of the system, which is simulated by a specially parametrized MM force field that utilizes potential-derived charges (PDC).[33] The active center contains the central Ti cation with four neighboring silica tetrahedral groups. The QM cluster is terminated by capping monovalent oxygen centers O* atoms, constructed in analogy to the pseudobond approach used previously in the QM/MM modeling of enzymes.[39] In the covEPE scheme, such bond-capping border centers O* are located at anionic positions of oxygen atoms of the silicate framework. In this way, the method overcomes the drawback of conventional QM/MM methods with additional hydrogen centers as link atoms between the QM and MM regions.[40−42] The QM and MM regions interact via direct short-range forces, and they also respond self-consistently to long-range polarization effects. The long-range interaction of the lattice ions with the QM cluster is represented efficiently by the field of a set of point charges located on a sphere that encompassed the QM cluster.[43]

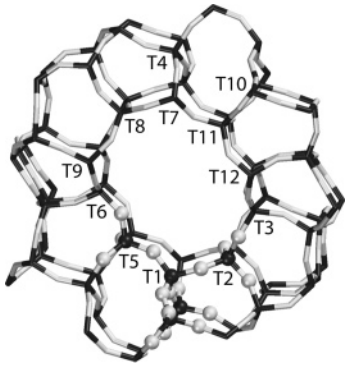

Figure 1. Sketch of the orthorhombic MFI structure with all 12 crystallographically distinct T sites labeled. As an example, the atoms of the QM cluster model containing 5T sites centered at position T1 are indicated as spheres.

Thus, the covEPE method completely and explicitly includes both electrostatic and mechanical interactions of the QM cluster and its surroundings. It affords a variational treatment of an energy expression that includes all degrees of freedom of both QM and MM regions. Furthermore, the covEPE method accounts for the polarization of the environment by the QM cluster, which is lacking in many popular QM/MM schemes that are used for modeling systems with covalent Si−O bonds. A detailed description of the covEPE method for zeolites with infinite and finite Si/Al ratios, including the force fields used, can be found in refs 33 and 35, respectively.

2.2. Computational Details. The QM calculations were carried out with the linear combination of Gaussian-type orbital fitting function density functional method (LCGTO−FF-DF)[44] as implemented in the PARAGAUSS program.[45,46] We used the gradient-corrected exchange-correlation functional suggested by Becke (exchange)[47] and Perdew (correlation).[48] The Kohn−Sham orbitals were represented by Gaussian-type basis sets: (6s1p) → (4s1p) for H, (9s5p1d) → (5s4p1d) for O, (12s9p2d) → (6s4p2d) for Si, and (15s11p6d) → (6s5p3d) for Ti.[49] All contractions were of generalized atomic form. For calculating the Hartree contribution of the electron−electron interaction, an auxiliary basis set is employed to represent the electronic charge density.[44] The exponents of the auxiliary basis set were constructed by scaling the exponents of the orbital basis, a standard set of five p-type and five d-type polarization exponents was added on each atomic center.[50] The exchange-correlation energy and the matrix elements of the exchange-correlation potential were evaluated by an accurate numerical integration.[51,52] The structure of the system was optimized using analytical energy gradients[53] and the BFGS Hessian update scheme.[54]

We applied the covEPE method[33] to investigate the nonrandom distribution of titanium atoms in TS-1 zeolite. For each of the 12 crystallographically distinct T sites of MFI zeolite structure (see Figure 1), the QM region of the covEPE model $T[OSiO^*_3]_4$ with T = Si or Ti contained 5T centers. The main discussion in Section 3 is based on these 5T QM models, unless stated differently. In fact, to test the convergence of the results with increasing size of the QM region, we also carried out calculations on selected T sites using extended QM clusters $T[OSiO^*_3]_3-OSi[OSiO^*_3]_3$ with 8 T atoms. To construct these larger models, three border O* centers in one of four $OSiO^*_3$ units of the 5T model QM clusters were replaced by $OSiO^*_3$ groups. These enlarged clusters are built around crystallographic positions T2, T3, and T12, which have been determined as sites with the smallest, a medium, and the highest substitution energies of Ti (see below). The environment of the 5T and 8T QM clusters was represented as siliceous MFI structure, using a force field described previously.[33] The model systems generated in this way correspond to a zeolite with a very high Si/Ti ratio. The long-range steric bulk constraint of the zeolite lattice was taken into account by fixing all centers of the MM region (including T and O centers), which are at least 1.5 nm from any atomic center of the QM cluster.

We used two criteria to measure the energy preference for the substitution of Si by Ti at a certain T atom position, the relaxation energy, ΔE_{rel}, and the substitution energy, ΔE_{sub}. The relaxation energy characterizes the flexibility of the crystallographic position under consideration and is defined as the difference between the total energies of the optimized structure containing Ti, $E^{opt}(Ti)$, and the structure with Ti incorporated in the fixed framework as optimized for the pure silicalite structure, $E^{fix}(Ti)$

$$\Delta E_{rel} = E^{opt}(Ti) - E^{fix}(Ti)$$

The substitution energy measures the energy gained by substituting Si with Ti at a given T atom position and is defined as the reaction energy of the virtual reaction $Si(MFI) + Ti(OH)_4 \rightarrow Ti(MFI) + Si(OH)_4$, calculated as

$$\Delta E_{sub} = E^{opt}(Ti) - E^{opt}(Si) + E[Si(OH)_4] - E[Ti(OH)_4]$$

Here, the last two terms are the same for all crystallographic positions.

3. Results and Discussion

Internal cavities of the MFI zeolite framework comprise two topologically different channels, straight and zigzag intersecting. This zeolite structure contains 12 crystallographically distinct T sites, T1−T12.[25,26] Sites T1−T3, T5−T9, T11, and T12 are located only at the walls of straight channels, whereas the walls of zigzag channels comprise all T sites, including T4 and T10. The positions of all 12 T sites in MFI are illustrated in Figure 1.

3.1. Optimized Geometry of Siliceous T Sites. The structures of the twelve different Si-centered embedded clusters were optimized to produce the reference energies, $E^{opt}(Si)$, of the clean nondoped MFI material. In Table 2, we collect average bond distances and bond angles for each of the 12 T sites of a purely siliceous lattice of MFI structure, optimized with a periodic supercell MM approach and the hybrid QM/MM covEPE method. The reported parameters are averaged over all values calculated at each crystallographic T site. For the 8T QM clusters built around positions T2, T3, and T12, these averaged values differ from the corresponding results for 5T clusters at most by 1 pm or 1°, respectively.

As seen from Table 2, the average calculated Si−O distances vary only within about 1 pm, both at the MM and the QM/MM level. The individual Si−O bond lengths (four at each T site) are also very similar (see the Supporting Information). Overall, the Si−O bond distances, calculated with the covEPE method to vary from 163.1 to 163.8 pm, are about 2 pm longer than the experimental Si−O distances in MFI zeolites.[26] Such a slight overestimation of bond lengths is typical for the gradient-corrected exchange-correlation functional[55] applied in the present DF calculations. Typically, Si−O bond lengths in zeolites, calculated with different quantum chemical methods, deviate up to 5 pm from the crystallographic values,[56] depending on the level of the method applied and the parameters chosen. For example, Hartree−Fock (HF) calculations give Si−O distances

TABLE 2: Average T−O Bond Distances, T−Si Distances, and T−O−Si Bond Angles of All T Sites from MM Simulations of Pure Silicalite MFI and covEPE Calculations on Ti Centers of TS-1 from 5T and Extended 8T (in Parentheses) Embedded QM Models

		MFI, T = Si		TS-1, T = Ti
		MM	covEPE	covEPE
T−O, pm	T1	162	164	182
	T2	162	163 (163)	181 (181)
	T3	163	163 (164)	181 (181)
	T4	163	163	181
	T5	163	164	182
	T6	163	164	182
	T7	162	164	182
	T8	162	163	181
	T9	162	163	181
	T10	162	163	181
	T11	163	164	182
	T12	163	164 (164)	182 (182)
T−Si, pm	T1	310	312	321
	T2	314	315 (315)	326 (327)
	T3	311	313 (314)	323 (327)
	T4	312	314	323
	T5	309	311	323
	T6	309	311	320
	T7	309	310	319
	T8	314	315	327
	T9	311	315	325
	T10	309	311	322
	T11	310	310	322
	T12	312	313 (312)	322 (322)
T−O−Si, degree	T1	146	144	136
	T2	150	148 (149)	141 (143)
	T3	147	145 (146)	138 (143)
	T4	147	146	141
	T5	145	142	138
	T6	145	143	135
	T7	144	141	134
	T8	149	148	142
	T9	147	146	140
	T10	144	143	137
	T11	145	141	137
	T12	147	145 (144)	137 (138)

around 162 pm, whereas accounting for electron correlation at the MP2 level results in longer distances, up to 164 pm.[56] Calculations with periodic boundary conditions using gradient-corrected density functionals give Si−O distances in the same range, 161−164 pm.[57−59]

Si−O−Si angles, calculated at the covEPE level, vary from 141° to 148° (Table 2). The corresponding averaged experimental crystallographic results[26] for different T sites fall in the interval from 152° to 161°. The slight underestimation of bond angles in the present covEPE calculations is also attributed to the gradient-corrected density functional used; note that the bond angles calculated at the MM level are larger than those obtained in the QM/MM calculations (Table 2).

The average Si−Si distances calculated with the covEPE method, 309−313 pm, are in good agreement with the experimental averaged value of ∼310 pm.[26,60]

3.2. Geometry of Ti-Containing T Sites. The average geometric parameters of Ti-containing 5T clusters, as obtained from our covEPE calculations, are also listed in Table 2. As the most prominent effect, the average T−O bond lengths increase by about 18 pm upon Ti insertion into the framework of the MFI zeolite. The Ti−O distances, calculated at 181−182 pm, are in good agreement with the experimental values derived from EXAFS results, 181 ± 1 pm.[10] The calculations with 8T clusters gave exactly the same averaged Ti−O distances as the corresponding 5T QM cluster models (Table 2).

Similar values have been obtained in DF calculations of isolated clusters with different steric restrictions, 178−184 pm,[19,21,22] in HF calculations of TS-1 with the QM-pot and the ONIOM method, 179−181 pm,[20,24] and with periodic HF calculations of Ti containing chabazite,[61] 178−180 pm.

The elongation of the T−O bond distance upon Ti incorporation in MFI causes a local expansion and, consequently, a deformation of the MFI framework, resulting in significant changes of the T−O−Si angles compared to corresponding angles in the siliceous structure. The calculated individual Ti−O−Si angles are by about 10° smaller and they vary in a wider range, 124−150°, compared to the Si−O−Si angles, 135−153° (see the Supporting Information). The calculated trend toward a wider range of T−O−Si bond angles (due to a reduction of some angles while the largest angles remain unchanged) is in good agreement with the trends derived from the EXAFS data, with T−O−Si angles of 152−161° in pure silicalite and 140−160° in the Ti-containing MFI material.[9] (The averaged values of the Ti−O−Si angles for the 8T QM clusters with Ti at positions T2, T3, and T12 differ from the values of corresponding 5T clusters by 2°, 5°, and 1°, respectively).

Because the Ti−O−Si angles are sensitive to the type and rigidity of the zeolite framework in which the central TiO_4 tetrahedron is embedded, there are only a few other computational studies that allow a comparison with our *systematic* embedding modeling. However, such comparison has to remain rather limited because these other calculations were either based on isolated clusters or address Ti centers in zeolite frameworks that are not relevant to the real TS-1 material. A QM-pot study of TS-1[20] would be suitable for a comparison with our results, but unfortunately it does not report the values of the T−O−T angles. Hybrid QM/MM modeling of the Ti-containing MFI zeolite with the ONIOM approach[23] suggested rather small Ti−O−Si angles, 116−132°, that likely result from limited relaxation of the Si centers close to the titanium center represented by the minimal TiO_4 QM cluster model. The positions of the Si centers in question were optimized at the MM level only; furthermore, framework centers in subsequent shells were not relaxed at all from their positions in the pure silica MFI structure. Mild structural constraints (which allowed all T and O centers to relax) within an ONIOM scheme at the QM(B3LYP):QM(HF) level[62,63] yielded larger Ti−O−Si angles for the T1 site[64] of the MFI lattice; these angles varied over a wide range, from 135° to 173°.[24] Some uncertainty in these ONIOM studies arises from the fact that in both cases the zeolite framework, effectively of infinite extension, was represented by relatively small model clusters.

As a result of the extension of the Ti−O bonds, the interatomic Ti−Si distances are also enlarged in the Ti form of the zeolite, on average by about 10 pm, compared to the Si−Si distances in the pure silica form. This bond elongation is about half of that of the Ti−O bonds because the deformation of the Ti−O−Si angles partially compensates for the expansion of the "central" TiO_4 tetrahedron. The average calculated Ti−Si distances at each T site vary from 319 pm (T7) to 327 pm (T8) in the 5T QM models. Extension of the QM cluster to 8T models for selected T sites showed that these distances can be 1−4 pm larger (Table 2), thus approaching the experimental range of Ti−Si distances, 321−337 pm.[9] The B3LYP:HF ONIOM calculations[24] predicted a wider range of Ti−Si distances, 320−344 pm; this is in line with the larger scattering of Ti−O−Si angles of that computational approach (see above).

TABLE 3: Calculated Relaxation Energies,[a] ΔE_{rel}, and Substitution Energies,[b] ΔE_{sub}, (kJ/mol) when Si Atoms at the 12 Crystallographically Unique T Sites of MFI Zeolite are Replaced by Ti Atoms from 5T and Extended 8T (in Parentheses) Embedded QM Models

T sites	ΔE_{rel}	ΔE_{sub}
T1	−245	−90
T2	−252	−88 (−87)
T3	−248	−95 (−91)
T4	−250	−93
T5	−247	−99
T6	−244	−89
T7	−246	−97
T8	−262	−97
T9	−252	−92
T10	−251	−92
T11	−247	−93
T12	−249	−107 (−98)

[a] Ti incorporation in the fixed MFI framework as optimized for the pure silicalite structure: $\Delta E_{rel} = E^{opt}(Ti) - E^{fix}(Ti)$ [b] Reaction energy of the virtual reaction $Si(MFI) + Ti(OH)_4 \rightarrow Ti(MFI) + Si(OH)_4$, calculated as $\Delta E_{sub} = E^{opt}(Ti) - E^{opt}(Si) + E[Si(OH)_4] - E[Ti(OH)_4]$.

3.3. Relaxation and Substitution Energies. The substitution and relaxation energies for all 12 T sites of MFI zeolite are given in Table 3. The *substitution energy* measures the energy gained by a virtual substitution reaction where at the given T atom position a Si center is replaced by Ti (see Section 2.2). If the distribution of the Ti centers in the MFI structure is determined by the thermodynamic stability of the final adsorbate-free zeolite framework, then the substitution energy will be an appropriate criterion for the preferential siting of Ti. The substitution energies of the 12 T sites vary in a narrow range of 19 kJ/mol, from −88 to −107 kJ/mol. A negative value of the substitution energy implies that Ti substitution in an MFI framework is energetically feasible when $Si(OH)_4$ and $Ti(OH)_4$ species are considered as energy references. With −107 kJ/mol, T12 is the most preferred site, followed by T5, T7, and T8, which are characterized by results that are about 10 kJ/mol lower in absolute value. The lowest substitution energies (by absolute value) were calculated for sites T2 and T6. The same trend in the substitution energies was also determined for the extended 8T QM cluster models, applied at selected sites, T2, T3, and T12, namely, with the smallest, a medium, and the highest substitution energies of Ti, respectively, for 5T models. The calculations with 8T models yielded a smaller variation of the substitution energies. For 8T cluster models, the substitution energies of T12 and T2 differed by 11 kJ/mol (Table 3), slightly smaller than the difference for the 5T models, 19 kJ/mol.

As discussed in the previous section, there are significant changes in T−O bond lengths, T−Si distances, and T−O−Si angles upon Ti incorporation in zeolite MFI. Hence, one can expect that accommodation of a Ti atom in the zeolite structure results in a large relaxation of the framework. As an estimate of this relaxation, we consider the *relaxation energy*, ΔE_{rel}, at each crystallographic position, defined as the difference between the total energies of the optimized structure containing Ti and the structure with Ti incorporated in the fixed framework as optimized for the pure silica structure. Thus, the relaxation energy reflects the local flexibility of the framework at a given crystallographic position and, consequently, the ability of the local zeolite structure to accommodate a larger Ti(IV) center instead of a Si(IV) center; the corresponding covalent radii differ by about 25 pm.

The relaxation energies vary from −244 kJ/mol to −262 kJ/mol; with 18 kJ/mol, this interval is essentially of the same size as that of the substitution energies. The largest energy release upon relaxation is calculated at the T8 position; the relaxation energies of the other eleven positions vary only within 8 kJ/mol (Table 3). The smallest values for the energy release upon relaxation were determined for sites T6 and T1, which may be considered as the most rigid sites with respect to introduction of the larger Ti atoms. However, the large (absolute) value of ΔE_{rel} may also mean that Ti substitution at T8 requires a stronger relaxation of the surrounding framework to accommodate the Ti center.

3.4. Implications for the Preferential Siting of Ti Atoms in TS-1. On the basis of the energy changes calculated for the substitution of Ti as described above, we may conclude that T12, T5, T7, and T8 are thermodynamically most preferential sites for Ti substitution in the MFI structure. Under conditions of thermal equilibrium, the obtained energy differences among the calculated ΔE_{sub} values translate into relative populations of the 12 crystallographic positions where at room temperature 92% of the Ti atoms occupy site T12, followed by 4% at T5. At 448 K, a temperature typical for the synthesis of the material,[3,4] the population of the T12 site would be reduced to 71% and the majority of the remaining Ti centers would be distributed at T5 with 8%, and at T7 and T8 positions with 5% each; population at other sites would be 1−2%. Following these considerations, one should expect that experimental studies would observe Ti substitution mainly at the T12 position if the distribution of Ti centers in the MFI framework were determined by the thermodynamic stability only. However, as can be seen in Table 1, different experimental studies suggest different preferential positions of Ti in zeolite TS-1. Our results are in partial agreement with two of the five experimental studies referenced, which indicate that the T12 position is indeed among those populated most frequently.[8,29] However, the energy difference between Ti sites that we calculated, 19 kJ/mol, is rather small and one may expect that other factors can also affect the Ti distribution, such as (i) the thermodynamic stability of the product synthesized, which contains sorbed species inside the zeolite cavities, likely close to Ti centers, for example, water[20] or H_2O_2 molecules, (ii) the thermodynamic stability of Ti-containing oligomer species formed during synthesis and suitable for incorporation only in certain positions of the framework, and (iii) differences in kinetic limitations for incorporating Ti ions in different crystallographic positions during the synthesis of the material.

On the basis of the substitution energies of the 12 T sites obtained by semiempirical PM3 calculations, Hijar et al.[29] also found large deviations between simulations and their experimental observations. Moreover, they were also not able to rationalize their experimental results if they accounted for the presence of the structure-directing templates. They suggested that the Ti distribution in the framework be governed by kinetic factors during the formation of the zeolite framework.[29] An alternative explanation for the discrepancies among the different studies of the Ti location in TS-1 could be Si vacancies in the framework that are able to influence the distribution of Ti centers considerably,[30] especially if the defects are located in the vicinity of the Ti centers.

4. Conclusions

We have studied the preferential siting of Ti centers in TS-1 zeolite using a hybrid QM/MM approach based on a density functional implementation of the covEPE cluster-embedding method. The covEPE method affords a smooth embedding of the QM cluster in the surrounding framework because of an especially parametrized force field that simulates the MM

environment and allows an appropriate design of the QM/MM border region. Adequate modeling of environmental effects in the covEPE approach has been corroborated by the stability of the results upon increasing the size of the QM region. Using this method, we have calculated the local structure of each of the 12 crystallographically different T sites of MFI and we have determined the substitution energy of Ti to quantify the preferential siting of Ti. We have shown that incorporation of Ti atoms at tetrahedral sites of a siliceous MFI structure involves significant local changes in the lattice structure that are due mainly to longer T−O bonds, elongated from about 163.5 pm to 181.5 pm. The calculated local geometry, such as the Ti−O bond lengths and Ti−Si distances, are in very good agreement with the experimental results.

Among the 12 crystallographic T positions, T8 was found to be the most flexible; the obtained relaxation energy for this position is about 10 kJ/mol larger than the relaxation energies calculated for the other sites. By this criterion, these sites exhibit a comparable rigidity because the corresponding relaxation energies vary within only 8 kJ/mol.

The calculated substitution energies of Ti at different T sites suggest that incorporation of isolated Ti centers into the MFI framework is energetically favorable and that T12 is the preferred position for Ti substitution. The calculated relative substitution energies translate into thermal Ti populations of the different crystallographic sites where at 448 K about 70% of the Ti centers would occupy T12 sites. In other words, if the Ti distribution in the framework were governed by the thermodynamic stability of the final material, then the experimental studies should observe mainly Ti at this position. Apparently, this is not the case as indicated by the results of various experimental investigations. Therefore, we conclude that the distribution of Ti centers in TS-1 is not determined by the stability of the pure TS-1 framework but rather by other thermodynamic or kinetic factors. An important step in determining these factors would be a concerted effort of several experimental groups to synthesize TS-1 material under standardized conditions and to apply various analytical methods on one and the same sample of TS-1. These studies should be supplemented by focused theoretical modeling efforts.

Acknowledgment. R.C.D. thanks the Alexander von Humboldt Foundation for a research fellowship. E.A.I.S. gratefully acknowledges an individual grant of the Krasnoyarsk Regional Scientific Foundation (Grant 15G127). This work was also supported by Deutsche Forschungsgemeinschaft, Fonds der Chemischen Industrie, and the Bulgarian National Science Council.

Supporting Information Available: Calculated geometry parameters of the models of the 12 crystallographically unique positions of pure silica MFI and Ti-substituted MFI. This material is available free of charge via the Internet at http://pubs.acs.org.

References and Notes

(1) Bellussi, G.; Rigutto, M. *Stud. Surf. Sci. Catal.* **1994**, *85*, 177.
(2) Hadjiivanov, K. I.; Vayssilov, G. N. *Adv. Catal.* **2002**, *47*, 307.
(3) Taramasso, M.; Perego, G.; Notari, B. U.S. Patent 4410501, 1983.
(4) Notari, B. *Adv. Catal.* **1996**, *41*, 253.
(5) Vayssilov, G. N. *Catal. Rev.—Sci. Eng.* **1997**, *39*, 209, and references therein.
(6) Millini, R.; Previde Massara, E.; Perego, G.; Bullussi, G. *J. Catal.* **1992**, *137*, 497.
(7) Lamberti, C.; Bordiga, S.; Arduino, D.; Zecchina, A.; Geobaldo, F.; Spano, G.; Genoni, F.; Petrini, G.; Carati, A.; Villain, F.; Vlaic, G. *J. Phys. Chem. B* **1998**, *102*, 6382.
(8) Lamberti, C.; Bordiga, S.; Zecchina, A.; Carati, A.; Fitch, A. N.; Artioli, G.; Petrini, G.; Salvalaggio, M.; Marra, G. L. *J. Catal.* **1999**, *183*, 222.
(9) Gleeson, D.; Sankar, G.; Catlow, C. R. A.; Thomas, J. M.; Spano, G.; Bordiga, S.; Zecchina, A.; Lamberti, C. *Phys. Chem. Chem. Phys.* **2000**, *2*, 4812.
(10) Bordiga, S.; Coluccia, S.; Lamberti, C.; Marchese, L.; Zecchina, A.; Boscherini, F.; Buffa, F.; Genoni, F.; Leofanti, G.; Petrini, G.; Vlaic, G. *J. Phys. Chem.* **1994**, *98*, 4125.
(11) Blasco, T.; Camblor, M.; Corma, A.; Perez-Parriente, J. *J. Am. Chem. Soc.* **1993**, *115*, 11806.
(12) Zecchina, A.; Spoto, G.; Bordiga, S.; Ferrero, A.; Petrini, G.; Padovan, M.; Leofanti, G. *Stud. Surf. Sci. Catal.* **1991**, *69*, 251.
(13) Millini, R.; Perego, G.; Seiti, K. *Stud. Surf. Sci. Catal.* **1994**, *84*, 2123.
(14) de Man, A. J. M.; Sauer, J. *J. Phys. Chem.* **1996**, *100*, 5025.
(15) Oumi, Y.; Matsuba, K.; Kubo, M.; Inui, T.; Miyamoto, A. *Microporous Mater.* **1995**, *4*, 53.
(16) Yudanov, I. V.; Gisdakis, P.; Divalentin, C.; Rösch, N. *Eur. J. Inorg. Chem.* **1999**, 2135.
(17) Smirnov, K. S.; van de Graaf, B. *Microporous Mater.* **1996**, *7*, 133.
(18) Njo, S. L.; van Koningsveld, H.; van de Graaf, B. *J. Phys. Chem. B* **1997**, *101*, 10065.
(19) Sinclair, P. E.; Sankar, G.; Catlow, C. R. A.; Thomas, J. M.; Maschmeyer, T. *J. Phys. Chem. B* **1997**, *101*, 4232.
(20) Ricchiaridi, G.; de Man, A.; Sauer, J. *Phys. Chem. Chem. Phys.* **2000**, *2*, 2195.
(21) Munakata, H.; Oumi, Y.; Miyamoto, A. *J. Phys. Chem. B* **2001**, *105*, 3493.
(22) Vayssilov, G. N.; van Santen, R. A. *J. Catal.* **1998**, *175*, 170.
(23) Atoguchi, T.; Yao, S. *J. Mol. Catal. A* **2003**, *191*, 281.
(24) Damin, A.; Bordiga, S.; Zecchina, A.; Lamberti, C. *J. Chem. Phys.* **2002**, *117*, 226.
(25) http://www.iza-structure.org/databases.
(26) van Koningsveld, H.; Jansen, J. C.; van Bekkum, H. *Zeolites*, **1990**, *10*, 235.
(27) Marra, G. L.; Artioli, G.; Fitch, A. N.; Milanesio, M.; Lamberti, C. *Microporous Mesoporous Mater.* **2000**, *40*, 85.
(28) Lamberti, C.; Bordiga, S.; Zecchina, A.; Artioli, G.; Marra, G.; Spanò, G. *J. Am. Chem. Soc.* **2001**, *123*, 2204.
(29) Hijar, C. A.; Jacubinas, R. M.; Eckert, J.; Henson, N. J.; Hay, P. J.; Ott, K. C. *J. Phys. Chem. B* **2000**, *104*, 12157.
(30) Henry, P. F.; Weller, M. T.; Wilson, C. C. *J. Phys. Chem. B* **2001**, *105*, 7452.
(31) Sastre, G.; Corma, A. *Chem. Phys. Lett.* **1999**, *302*, 447.
(32) Perego, G.; Bellussi, G.; Corno, C.; Taramasso, M.; Buonomo, F. *Stud. Surf. Sci. Catal.* **1986**, *28*, 129.
(33) Nasluzov, V. A.; Ivanova, E. A.; Shor, A. M.; Vayssilov, G. N.; Birkenheuer, U.; Rösch, N. *J. Phys. Chem. B* **2003**, *107*, 2228.
(34) Catlow, C. R. A.; Mackrodt, W. C. In *Computer Simulations of Solids*, *Lecture Notes in Physics*; Catlow, C. R. A., Mackrodt W. C., Eds.; Springer: Berlin, **1982**; Vol. 166, p 3.
(35) Ivanova Shor, E. A.; Shor, A. M.; Nasluzov, V. A.; Vayssilov, G. N.; Rösch, N. *J. Chem. Theory Comput.* **2005,** *1*, 459.
(36) Schneider, W. F.; Hass, K. C.; Miletic, M.; Gland, J. L. *J. Phys. Chem. B* **2002**, *106*, 7405.
(37) Grey, T.; Gale, J.; Nicholson, D.; Artocho, E.; Soler, J. *Stud. Surf. Sci. Catal.* **2000**, *128*, 89.
(38) Whitmore, L.; Sokol, A. A.; Catlow, C. R. A. *Surf. Sci.* **2002**, *498*, 135.
(39) Zhang, Y.; Lee, T.-S.; Yang, W. *J. Chem. Phys.* **1999**, *110*, 46.
(40) Eichler, U.; Kölmel, C. M.; Sauer, J. *J. Comput. Chem.* **1996**, *18*, 463.
(41) Sherwood, P.; de Vries, A.; Collins, S. J.; Greatbanks, S. P.; Burton, N. A.; Vincent, M. A.; Hiller, I. H. *Faraday Discuss.* **1997**, *106*, 79.
(42) Shoemaker, J. R.; Burggraf, L. W.; Gordon, M. S. *J. Phys. Chem. A* **1999**, *103*, 3245.
(43) Stefanovich, E. V.; Truong, T. N. *J. Phys. Chem. B* **1998**, *102*, 3018.
(44) Dunlap, B. I.; Rösch, N. *Adv. Quantum Chem.* **1990**, *21*, 317.
(45) Belling, T.; Grauschopf, T.; Krüger, S.; Nörtemann, F.; Staufer, M.; Mayer, M.; Nasluzov, V. A.; Birkenheuer, U.; Hu, A.; Matveev, A. V.; Shor, A. M.; Fuchs-Rohr, M. S. K.; Neyman, K. M.; Ganyushin, D. I.; Kerdcharoen, T.; Woiterski, A.; Gordienko, A. B.; Majumder, S.; Rösch, N. *ParaGauss*, version 3.0; Technische Universität München, 2004.
(46) Belling, T.; Grauschopf. T.; Krüger, S.; Mayer, M.; Nörtemann, F.; Staufer, M.; Zenger, C.; Rösch, N. In *High Performance Scientific and Engineering Computing*, *Lecture Notes in Computational Science and Engineering*; Bungartz, H.-J., Durst, F., Zenger, C., Eds.; Springer: Heidelberg, Germany, 1999; Vol. 8, p 439.
(47) Becke, A. D. *Phys. Rev. A* **1988**, *38*, 3098.

(48) (a) Perdew, J. P. *Rhys. Rev. B* **1986**, *33*, 8822. (b) Perdew, J. P. **1986**, *34*, 7406.

(49) (a) Van Duijneveldt, F. B. *IBM Res. Report RJ* **1971**, 945. (b) *Gaussian Basis Sets for Molecular Calculations*; Huzinaga, S., Ed.; Elsevier: Amsterdam, 1984. (c) Veillard, A. *Theor. Chim. Acta* **1968**, *12*, 405. (d) Bär, M. R.; Sauer, J. *Chem. Phys. Lett.* **1994**, *226*, 405.

(50) Chung, S. C.; Krüger, S.; Pacchioni, G.; Rösch, N. *J. Chem. Phys.* **1995**, *102*, 3695.

(51) Pople, J. A.; Gill, P. M. W.; Johnson, B. G. *Chem. Phys. Lett.* **1992**, *199*, 557.

(52) Gill, P. M. W.; Johnson, B. G.; Pople, J. A. *Chem. Phys. Lett*. **1993**, *209*, 506.

(53) Nasluzov, V. A.; Rösch, N. *Chem. Phys.* **1996**, *210*, 413.

(54) Gill, P. E.; Murray, W.; Wright, M. H. *Practical Optimization*; Academic Press: New York, 1981.

(55) Görling, A.; Trickey, S. B.; Gisdakis, P.; Rösch, N. In *Topics in Organometallic Chemistry*; Brown, J., Hofmann, P., Eds.; Springer: Heidelberg, Germany, 1999; Vol. 4, p 109.

(56) Sierka, M.; Sauer, J. *Faraday Discuss.* **1997**, *106*, 41.

(57) Fois, E.; Gamba, A.; Spanò, E. *J. Phys. Chem. B* **2004**, *108*, 154.

(58) Zicovich-Wilson, C. M.; Dovesi, R. *J. Mol. Catal. A* **1997**, *119*, 449.

(59) Zicovich-Wilson, C. M.; Dovesi, R. *J. Phys. Chem. B* **1998**, *102*, 1411.

(60) Jentys, A.; Catlow, C. R. A. *Catal. Lett.* **1993**, *22*, 251.

(61) Damin, A.; Bordiga, S.; Zecchina, A.; Doll, K.; Lamberti, C. *J. Chem. Phys.* **2003**, *118*, 10183.

(62) We use the notation of Morokuma and co-workers,[63] namely, the HighLevelMethod:LowLevelMethod, to designate the combination of methods of a hybrid approach.

(63) Froese, R. D. J.; Morokuma, K. In *Encylopedia of Computational Chemistry*; Schleyer, P. v. R., Ed.; Wiley: Chichester, U.K., 1998; Vol. 2, p 1244.

(64) Only one T site has been modeled in ref 24.